Tri-Modal Biometric Fusion for Human Authentication by Tracking Differential Code Pattern

Aditya Nigam
School of Computing and Electrical Engineering
Indian Institute of Technology Mandi
175001 - India
aditya@iitmandi.ac.in

Phalguni Gupta
CSE Department
NITTTR, Salt Lake, Kolkata
700106 - India
pg@iitk.ac.in

***Abstract*—Human authentication can now be seen as a crucial social problem. In this paper a multimodal authentication system is presented which is highly reliable and fuses iris, finger-knuckle-print and palmprint image matching scores. Segmented ROI are preprocessed using *DCP* (Differential Code Pattern) to obtain robust corner features. Later they are matched using the *GOF* (Global Optical Flow) based dissimilarity measure. The proposed system has been tested on Casia Interval and Lamp iris, PolyU finger-knuckle-print and PolyU and Casia palmprint, public databases. The proposed system has shown good performance over all unimodal databases while over multimodal (fusion of all three) databases it has shown perfect performance (*i.e.* $CRR = 100\%$ with $EER = 0\%$).**

I. Introduction

Human authentication plays an important role in today's society. It can be realized through these three levels - Level 1 (Possession - token based), Level 2 (Knowledge - password based) and Level 3 (Biometrics - physiological and behavioral characteristics based). However, it is difficult to manage Level 1 and Level 2 security as both of them are not intrinsic user properties. But this is not the case with Level 3 security which is based on biometrics which can be considered as the science of personal authentication using physiological (*e.g.* fingerprint, face, iris, *etc.*) and behavioral characteristics of human beings (*e.g.* signature, gait,voice *etc.*).

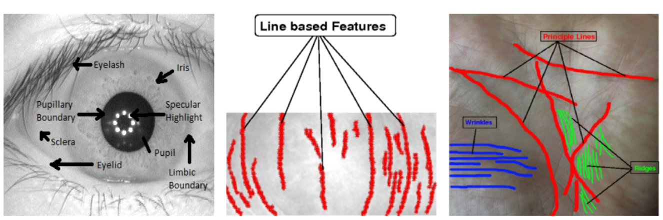

(a) Iris Anatomy (b) Knuckle Anatomy (c) Palmprint Anatomy

Fig. 1. Complex Anatomical structures of Iris, Knuckle and Palmprint

[a] Motivation : In this work iris, finger-knuckle-print and palmprint matching scores are fused for perfect performance.
[a] Iris : Thin circular diaphragm between cornea and lens is called as iris which has abundance of unique random micro-textures represented as crypts, furrows, ridges, corona, freckles and pigment spots [1], [2], as shown in Fig. 1[a]. Also it is a naturally well-protected biometric as compared to the other traits and is fairly robust to ageing.
[b] Finger-Knuckle-Print : The line like (*i.e.* knuckle lines) rich and unique [3], [4] pattern structures in vertical as well as horizontal directions exist over it, as shown in Fig. 1[b]. They are developed early and last very long with negligible amount of weir and tire. Hence its failure to enrollment rate is better than fingerprint in rural areas.
[c] Palmprint : The inner hand part is called as palm and region between fingers and wrist is termed as palmprint as shown in Fig. 1[c]. Pattern formation within this region is supposed to be stable as well as unique [5]. Huge amount of textures in the form of palm-lines, ridges, wrinkles *etc.* is available over palmprint.
[d] Multimodal Fusion: It has been observed experimentally that fusion of multiple biometric modalities facilitates the system to reject the imposters much more confidently [6], [7], [8], [9], [10], [11] and hence boosting the overall system performance significantly. Multimodal systems are much more relevant when the number of enrolled users is very large as false acceptance rate grows rapidly with database size. Also they can enable us to deal with missing trait and spoof vulnerability.
[b] Literature Review : Several uni-modal iris, finger-knuckle-print and palmprint based authentication systems are already proposed. But their performance got limited due to several trait specific challenges. Hence later research got diverted to fusing more than one biometric traits in pursuit of superior performance, which is termed as multimodal systems. Not much work has been reported in this area largely because of unavailability of true multi-modal biometric database. In [6], 2D discrete wavelets have been used to extract low dimensional features from iris and face. In [7], face and iris (left and right both) are fused using *SIFT* feature matching. In [8], iris and face are fused using PCA coefficients along with Daughman's gabor filter, features respectively. In [12], finger geometry and dorsal finger surface information are fused to improve the performance. In [13], 1D gabor filters are used to extract features from knuckle and palmprint, fused at score level. In [14], fusion of knuckle and palmprint is done using corner based local descriptors matched by cosine similarity. In [15], score level fusion is performed on palm and knuckleprints using phase only correlation (*POC*) function.

II. Proposed System

In this work raw images are segmented using algorithms presented in [2], [3], [5]. The sample image quality can also

This is pre-print version of paper accepted to NCVPRIPG 2015, IIT Patna.

play a significant role [16], [17]. The extracted region of interest (ROI) contains texture/line feature but generally is of poor contrast hence first enhancement is done.

[a] Enhancement : The ROI is divided into blocks of size 8×8 and mean of each block is considered as coarse illumination of that block. This mean is expanded to original block size. This estimated illumination of each block is subtracted from corresponding block of original image to obtain uniformly illuminated ROI. Then contrast is enhanced using Contrast Limited Adaptive Histogram Equalization ($CLAHE$). Finally, Wiener filter is applied to reduce constant power additive noise and the enhanced texture is obtained as shown in Figure 2.

[b] Differential Code Pattern (DCP) : The DCP pattern is used to transform ROI samples into a robust representations. The gradient (approximated by pixel difference) of any pixel is positive if it lies on an edge created due to light to dark shade (*i.e. high to low gray value*) transition. Hence all pixels can be divided into three classes of $+ve$, $-ve$ and *zero* gradient values. The *sobel* kernel fails to hold rotational symmetry; hence more consistent *scharr* kernels which are obtained by minimizing the angular error is applied. This gradient augmented information of each edge pixel can be more discriminative and robust. The transformation uses this information to calculate a 8-bit code (*i.e.* dcp) for each pixel. It uses gradient values of x- direction and y-direction of its 8 neighboring pixels to obtain DCP^v and DCP^h codes respectively as discussed below.

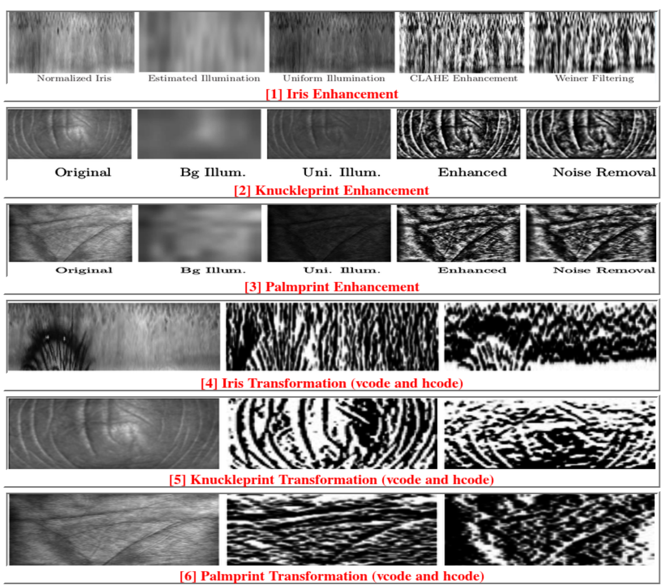

Fig. 2. Pre-processing of Iris, Knuckle and Palmprint, DCP^v and DCP^h codes

DCP code Generation : Let $P_{i,j}$ be the $(i,j)^{th}$ pixel of any biometric image P and $Neigh[k]$, $k = 1,2,...8$ are the gradients of 8 neighboring pixels centered at pixel $P_{i,j}$ obtained by applying x- direction or y- direction *scharr* kernel to obtain DCP^v and DCP^h respectively. Then the k^{th} bit of the 8-bit code (termed as dcp) is given by

$$dcp[k] = \begin{cases} 1 & \textbf{if } Neigh[k] > 0 \\ 0 & \textbf{otherwise} \end{cases} \tag{1}$$

$$DCP(x,y) = \sum_{i=0}^{7} dcp[i] * 2^i \tag{2}$$

In DCP^v and DCP^h, every pixel is represented by its DCP value as shown in Fig. 2. The pattern of edges within a neighborhood is assumed to be robust; hence each pixel's DCP value is considered which is just an encoding of edge pattern of its 8-neighborhood.

[c] Feature Extraction : The corner features [18] are extracted from both DCP^v and DCP^h obtained from any sample ROI. The KL tracking [19] has been used to track the corner features in the corresponding images for matching two sample ROI. The KL tracking makes use of three assumptions, namely brightness consistency, temporal persistence and spatial coherency. Hence its performance depends completely on how well these three assumptions are satisfied. It can be safely assumed that these three assumptions are more likely to be satisfied while tracking is performed between features of same subject (genuine matching) and degrades substantially for others (imposter matching). Therefore, one can infer that the performance of KL tracking algorithm is good in genuine matching as compared to the imposter ones.

[iv] Matching : The direction of pixel motion which is termed as $optical\ flow$ of that pixel, can be computed by KL-tracking algorithm. A dissimilarity measure GOF (Global Optical Flow) has been proposed to estimate the KL-tracking performance. It checks these three quantities for each potential matching feature pair given by KL-tracking algorithm.

[a] Vicinity Constraints : Euclidean distance between any corner and its estimated tracked location should be less than or equal to an empirically selected threshold (T_d). High threshold value signifies more translation and vise-versa.

[b] Patch-wise Dissimilarity : Pixel-wise sum of absolute difference between a local patch centered at current corner and that of its estimated tracked location patch should be less than or equal to an empirically selected threshold (T_e).

[c] Correlation Bound : Phase only correlation (POC) [15] between a local patch centered at any feature and that of its estimated tracked location patch should be at-least equal to an empirically selected threshold T_{cb}.

However, all tracked corner features may not be the true matches because of noise, local non-rigid distortions in the biometric samples and also less difference in inter class matching and more in intra-class matching. Hence, the direction of pixel motion (*i.e* optical flow) for each pixel is used to prune out some of the false matching corners. It can be noted that true matches have the optical flow which can be aligned with the actual affine transformation between two images that are being matched. The estimated optical flow angle is quantized into eight directions and the most consistent direction is the one which has the largest number of successfully tracked corner features. Any corner matching pair (*i.e* corner and its corresponding corner) having optical flow direction other than the most consistent direction is considered as false matching pair and has to be discarded.

Matching Algorithm : Given DCP^v and DCP^h of two samples, Algorithm 1 can be used to compute a dissimilarity score using GOF measure. Corresponding DCP^v codes are matched to obtain the vertical matching score while the respective DCP^h are matched to generate horizontal matching score. The corner features that are having their tracked position and local patch dissimilarity within the thresholds are considered as successfully tracked. Since both S_a to S_b and S_b to S_a

matching are considered, four sets of successfully tracked corners are computed *viz.* $stc^v_{AB}, stc^h_{AB}, stc^v_{BA}$ and stc^h_{BA}. The optical flow for each successfully tracked corner is quantized into eight bins at an interval of $\frac{\pi}{8}$. Four histograms (of eight bins each) are obtained, one for each set of successfully tracked corners represented by $H^v_{AB}, H^h_{AB}, H^v_{BA}$ and H^h_{BA}. The maximum value in each histogram represents the total number of corners having consistent optical flow and these are represented as $cof^v_{AB}, cof^h_{AB}, cof^v_{BA}$ and cof^h_{BA}. Finally they are normalized by the total number of corners and are converted into horizontal and vertical dissimilarity scores. The final score, $GOF(S_a,S_b)$ is obtained by using sum rule of horizontal and vertical matching scores. Such a fusion can significantly boost-up the performance of the proposed system because some of the images are having more discrimination in vertical direction while others have it in horizontal direction.

Algorithm 1 $GOF(S_a,S_b)$

Require:
(a) Two DCP^v codes I^v_A, I^v_B of samples S_a, S_b respectively.
(b) Two DCP^h codes I^h_A, I^h_B of samples S_a, S_b respectively.
(c) N^v_a, N^v_b, N^h_a and N^h_b are the number of corners in I^v_A, I^v_B, I^h_A, and I^h_B respectively.

Ensure: Return $GOF(S_a,S_b)$.

1: Track all the corners of I^v_A inI^v_B and that of I^h_A in I^h_B.
2: Obtain the set of corners successfully tracked in DCP^v tracking (*i.e.* stc^v_{AB}) and DCP^h tracking (*i.e.* stc^h_{AB}) that have their tracked position within T_d and their local patch dissimilarity under T_e with their patch-wise correlation more than T_{cb}.
3: Similarly compute successfully tracked corners of I^v_B in I^v_A (*i.e.* stc^v_{BA}) as well as I^h_B in I^h_A (*i.e.* stc^h_{BA}).
4: Quantize optical flow direction for each successfully tracked corners into eight directions (*i.e.* at an interval of $\frac{\pi}{8}$) and obtain 4 histograms $H^v_{AB}, H^h_{AB}, H^v_{BA}$ and H^h_{BA} using these four corner set $stc^v_{AB}, stc^h_{AB}, stc^v_{BA}$ and stc^h_{BA} respectively.
5: For each histogram, out of 8 bins the bin (*i.e.* direction) having the maximum number of corners is considered as the consistent optical flow direction. The maximum value of each histogram is termed as corners having consistent optical flow represented as $cof^v_{AB}, cof^h_{AB}, cof^v_{BA}$ and cof^h_{BA}.
6: $gof^v_{AB} = 1 - \frac{cof^v_{AB}}{N^v_a}$; $gof^v_{BA} = 1 - \frac{cof^v_{BA}}{N^v_b}$; [$DCP^v$ Matching]
7: $gof^h_{AB} = 1 - \frac{cof^h_{AB}}{N^h_a}$; $gof^h_{BA} = 1 - \frac{cof^h_{BA}}{N^h_b}$; [$DCP^h$ Matching]
8: **return** $GOF(S_a,S_b) = \frac{gof^v_{AB}+gof^h_{AB}+gof^v_{BA}+gof^h_{BA}}{4}$;

III. Experimental Analysis

The proposed system is tested on two publicly available CASIA V4 Interval [20] and Lamp [20] iris databases, two publicly available CASIA [20] and PolyU [21] palmprint databases along with the largest publicly available PolyU [21] finger-knuckle-print database. The CASIA V4 Interval database contains $2,639$ iris images collected from 395 distinct irises while the Lamp database contains $16,212$ images collected from 819 distinct irises. The PolyU Knuckleprint database consists of $7,920$ FKP images obtained from 660 distinct knuckleprints. The CASIA palmprint database has $5,502$ palmprints taken from 624 distinct palms while PolyU palmprint database has $7,752$ palmprint of 386 distinct palms.

The two iris databases are fused with two palmprint databases and one knuckleprint database. Hence, four chimeric multimodal databases are created *viz.* db1, db2, db3 and db4.

db1 : It consider all iris images of interval database belonging to all subjects. These iris samples are fused with first 349 subjects of knuckleprint (PolyU) and palmprint (CASIA) databases. First 3 images are considered for training while first 4 images of second session are used for testing.
db2 : It consider every iris image of all interval subjects. These iris samples are fused with first 349 subjects of knuckleprint (PolyU) and palmprint (PolyU) databases. First 3 images are considered for training while first 4 images of second session are considered as testing images.
db3 : It consider 8 palmprint images taken from all CASIA palmprint subjects. These palmprint of first 566 subjects are fused with knuckleprints (PolyU) and iris (Lamp) databases. First 4 images are considered for training while first 4 images of second session are used for testing.
db4 : It consider 12 palmprint images taken from all PolyU palmprint subjects. These palmprints are fused with first 386 subjects of knuckleprint (PolyU) and iris (Lamp) databases. For both knuckleprint and iris, first 6 images are used for training and first 6 of second session are used for testing.

[i] Testing Strategy : In order to test the proposed system a hard inter-session testing strategy is devised which is described as follows. Any system typically enrolls only one image per subject during the enrollment phase. Hence one training and one testing image per subject (*i.e* $1-Training$ and $1-Testing$) can be a suitable testing strategy for more general system setting. Also all training and testing images per subject are used to analyze the average system behavior. Multiple training images facilitate the identification and hence, affect CRR favorably. On the other hand, multiple image testing scenario is dependent upon the variability in the testing samples. If the database contains less variation and the subsequent testing samples are almost similar to each other than multiple testing images may effect the system performance favorably. But if the testing images are having more texture variation and are different to each other, than performance may be adversely affected. For every database, the case where only single testing image is used, it always considers the first image of the second session. But while for training, either under single or multiple image strategy, all possible combinations are considered and average results are reported in Table I.

[ii] Result Analysis : The proposed multimodal system is tested over four self created databases. The system parameters (*viz.* T_d, T_e, T_{cb}) for all three traits are chosen in order to maximize the system performance (in terms of CRR, EER) over a small validation set. One training and one testing along with all training and testing strategy are considered and four performance parameters *viz.* $FA =$ Falsely Accepted imposters, $FR =$ Falsely rejected genuine, $EER =$ Equal error rate and $CRR =$ Correct recognition rate are reported. One can observe from Table I that after fusion, results obtained for all databases under all different testing strategies tend to become almost perfect (*i.e.* $CRR = 100\%$ with $EER = 0\%$) hence ROC analysis has not been done. Moreover, one can also observe that with the increase in the number of training and testing

Biometric Traits ⇒				**Iris** (I)		**Knuckle** (K)		**Palmprint** (P)		**Fusion**	
Db Name	Testing Strategy	Total Genuine	Total Imposter	FA EER (%)	FR CRR (%)	FA EER (%)	FR CRR (%)	FA EER (%)	FR CRR (%)	FA EER (%)	FR CRR (%)
db1[I=Interval; K=PolyU; P=Casia]	1**Tr**-1**Test**	349	121452	240	0.66	1849	5	235.33	0.66	0	0
				0.19	99.80	1.47	97.80	0.19	99.90	0	100
db1 [I=Interval; K=PolyU; P=Casia]	3**Tr**-4**Test**	3657	1276293	1392	4	21923	63	3007	9	0	0
				0.10	100	1.72	99.67	0.24	99.91	0	100
db2 [I=Interval; K=PolyU; P=PolyU]	1**Tr**-1**Test**	349	121452	240	0.66	1849	5	617.66	1.66	0	0
				0.19	99.80	1.47	97.80	0.49	99.33	0	100
db2 [I=Interval; K=PolyU; P=PolyU]	3**Tr**-4**Test**	3657	1276293	1392	4	21923	63	4872	14	0	0
				0.10	100	1.72	99.67	0.38	99.91	0	100
db3 [I=Lamp; K=PolyU; P=Casia]	1**Tr**-1**Test**	566	319790	4970.33	8.66	6027.66	10.66	385.33	0.66	0	0
				1.54	97.29	1.88	97.17	0.11	99.94	0	100
db3 [I=Lamp; K=PolyU; P=Casia]	4**Tr**-4**Test**	9056	5116640	66217	117	99902	177	7912	14	0	0
				1.29	99.77	1.95	99.55	0.15	100	0	100
db4 [I=Lamp; K=PolyU; P=PolyU]	1**Tr**-1**Test**	386	148610	2435	6.33	2181	5.66	1026.6	2.66	0	0
				1.64	97.23	1.46	98.01	0.69	99.13	0	100
db4 [I=Lamp; K=PolyU; P=PolyU]	6**Tr**-6**Test**	13896	5349960	70833	184	87401	227	43504	113	385	1
				1.32	99.87	1.63	99.87	0.81	99.91	0.0071	100

TABLE I. PERFORMANCE PARAMETERS FOR UNI-MODEL AND CHIMERIC MULTIMODAL DATABASES ($db1, db2, db3$ & $db4$).

images, the genuine and the imposter matching are increased significantly that affect the performance of any unimodal system but the performance of each fused system remains almost invariant. Hence, one can also infer that the fusion of multiple traits introduces great amount of scalability with respect to system performance. More and more matching can be considered without much performance degradation. This is achieved because many uncorrelated traits are fused enhancing the uniqueness and discriminative power of combined sample.

IV. CONCLUSION

We have proposed a highly reliable multimodal authentication system using iris, finger-knuckle-print and palmprint images, fused at score level. The proposed system has been tested over public databases and has achieved perfect performance over chimeric multimodal (fusion of all three) databases.

REFERENCES

[1] K. W. Bowyer, K. Hollingsworth, and P. J. Flynn, “Image understanding for iris biometrics: A survey,” *Computer Vision and Image Understanding*, vol. 110, no. 2, pp. 281 – 307, 2008.

[2] A. Nigam and P. Gupta, “Iris recognition using consistent corner optical flow,” in *Asian Conference on Computer Vision, (ACCV)*, 2013, vol. 7724, pp. 358–369.

[3] L. Zhang, L. Zhang, D. Zhang, and H. Zhu, “Ensemble of local and global information for finger-knuckle-print recognition,” *Pattern Recognition*, vol. 44, no. 9, pp. 1990 – 1998, 2011.

[4] A. Nigam and P. Gupta, “Finger knuckleprint based recognition system using feature tracking,” in *Biometric Recognition*, 2011, pp. 125–132.

[5] G. Badrinath and P. Gupta, “Palmprint based recognition system using phase difference information,” *Future Generation Computer Systems*, vol. 28, pp. 287–305, 2010.

[6] B. Son and Y. Lee, “Biometric authentication system using reduced joint feature vector of iris and face,” in *Audio and Video Based Biometric Person Authentication*. LNCS - Springer, 2005, vol. 3546, pp. 513–522.

[7] A. Rattani and M. Tistarelli, “Robust multi-modal and multi-unit feature level fusion of face and iris biometrics,” in *Advances in Biometrics*. LNCS - Springer, 2009, vol. 5558, pp. 960–969.

[8] Z. Zhang, R. Wang, K. Pan, S. Li, and P. Zhang, “Fusion of near infrared face and iris biometrics,” in *Advances in Biometrics*. LNCS - Springer, 2007, vol. 4642, pp. 172–180.

[9] A. Nigam and P. Gupta, “Multimodal personal authentication system fusing palmprint and knuckleprint,” in *Emerging Intelligent Computing Technology and Applications*, 2013, vol. 375, pp. 188–193.

[10] A. Nigam and G. Phalguni, “Multimodal personal authentication using iris and knuckleprint,” in *Intelligent Computing Theory*, 2014, vol. 8588, pp. 819–825.

[11] A. Nigam and P. Gupta, “Designing an accurate hand biometric based authentication system fusing finger knuckleprint and palmprint,” *Neurocomputing*, vol. 151, Part 3, pp. 1120 – 1132, 2015.

[12] A. Kumar and C. Ravikanth, “Personal authentication using finger knuckle surface,” *IEEE Transactions on Information Forensics and Security*, vol. 4, no. 1, pp. 98–110, 2009.

[13] A. Meraoumia, S. Chitroub, and A. Bouridane, “Palmprint and finger-knuckle-print for efficient person recognition based on log-gabor filter response,” *Analog Integrated Circuits and Signal Processing*, vol. 69, pp. 17–27, 2011.

[14] L.-Q. Zhu and S.-Y. Zhang, “Multimodal biometric identification system based on finger-geometry, knuckleprint and palmprint,” *Pattern Recognition Letters*, vol. 31, no. 12, pp. 1641 – 1649, 2010.

[15] A. Meraoumia, S. Chitroub, and A. Bouridane, “Fusion of finger-knuckle-print and palmprint for an efficient multi-biometric system of person recognition,” in *IEEE International Conference on Communications (ICC)*, 2011, pp. 1–5.

[16] A. Nigam, A. T., and P. Gupta, “Iris classification based on its quality,” in *Intelligent Computing Theories*, 2013, vol. 7995, pp. 443–452.

[17] A. Nigam and P. Gupta, “Quality assessment of knuckleprint biometric images,” in *Image Processing (ICIP), 2013 20th IEEE International Conference on*, Sept 2013, pp. 4205–4209.

[18] J. Shi and Tomasi, “Good features to track,” in *Computer Vision and Pattern Recognition (CVPR)*. IEEE, 1994, pp. 593–600.

[19] B. D. Lucas and T. Kanade, “An Iterative Image Registration Technique with an Application to Stereo Vision,” in *International Joint Conference on Artificial Intelligence (IJCAI)*, 1981, pp. 674–679.

[20] CASIA, “The iris (interval,lamp) and palmprint databases,” http://biometrics.idealtest.org/#.

[21] PolyU, “The palmprint and knuckleprint database,” http://www4.comp.polyu.edu.hk/~biometrics/.